Available online at www.sciencedirect.com
SCIENCE DIRECT
International Journal of Mass Spectrometry 249–250 (2006) 199–205
International Journal of Mass Spectrometry
www.elsevier.com/locate/ijms

An infrared spectroscopic study of protonated and cationic indazole

Jos Oomens [a,*], Gerard Meijer [a,b], Gert von Helden [b]

[a] *FOM Institute for Plasma Physics "Rijnhuizen", Edisonbaan 14, 3439MN Nieuwegein, The Netherlands*
[b] *Fritz Haber Institut der Max Planck Gesellschaft, Faradayweg 4-6, D-14195 Berlin, Germany*

Received 26 October 2005; received in revised form 20 December 2005; accepted 20 December 2005
Available online 25 January 2006

Abstract

The mid-infrared vibrational spectra of the cationic and protonated forms of the molecule indazole ($C_7N_2H_6$) are recorded in the gas phase, applying the method of free electron laser induced multiple photon dissociation spectroscopy in a quadrupole ion trap. The spectra are compared to density functional theory calculations, which for the protonated species suggests that the proton attaches to the pyridine-like nitrogen atom. The spectrum of the indazole cation raises the question whether indazole undergoes an N1–N2 H atom shift upon ionization. The spectra for the charged species are further discussed in comparison with the spectrum of neutral indazole. Although the spectral range probed in this study, 600–1800 cm^{-1}, does not cover the hydrogen stretching modes, the spectra are found to be very distinct, indicating how a subtle change in electron distribution can have major effects on the vibrational spectrum of a conjugated system.

Keywords: Indazole; Cation; Protonated; Tautomerism; Infrared spectroscopy

1. Introduction

In recent years, there has been a growing interest in the spectroscopic investigation of biologically relevant molecules in the gas phase [1–12], aiming at a characterization of their intrinsic structural properties, free from any environmental effects. Particularly the "fingerprint" mid-infrared wavelength range of the spectrum is effective to obtain structural information. Elegant UV–IR pump-probe methods have been developed to obtain conformer specific infrared spectra. Systems studied include nucleic acid bases [5] and base pairs [1], amino acids [6,7], saccharides [8], small peptides [9–11], neurotransmitters [12], et cetera.

Evidently, protonation is a process of key biochemical interest. Obtaining infrared spectra of protonated species, however, involves the study of ionic species in the gas phase, and this is, in general, not a sinecure [13]. Several small, prototypical, protonated molecules such as H_3^+, H_3O^+, and HCO^+ [14] have been investigated with IR spectroscopy in the 1970s and 1980s. In these studies, mainly discharge and electron impact ionization sources have been used, which are not well suited for larger, biologically relevant molecules as they induce severe or even complete fragmentation of those species. The use of more gentle and/or mass-selective methods of ionization, inherently decreases the ion densities and therefore generally precludes the application of direct absorption spectroscopy. Recently, however, several spectroscopic studies of gas-phase protonated species have been reported [15–24], based mainly on infrared photo-dissociation spectroscopy. Among others, these studies have been very successful in determining the protonation site. In addition, IR spectra of some proton-bound dimers, most notably the protonated water dimer $H_5O_2^+$, have recently been reported [24–28]. Other recent exciting studies are the infrared spectrum of protonated methane (CH_5^+), obtained using laser induced reaction in a low-temperature ion trap [29], and the infrared spectra of multiply protonated proteins [30,31].

Initially, most of these studies were performed in the wavelength region around 3 μm (where table-top laser systems are widely available) as the hydrogen stretching modes in this range are obviously very sensitive to protonation. Since the coupling of ion trapping devices to infrared free electron lasers at our institute [32,33] as well as at Orsay, France [34], the mid/far-infrared range became accessible and multiple photon dissociation spectroscopy of several protonated systems has been reported [18,20,22,23,25,26]. Although not directly probing the H stretching modes, these experiments allow, in combination with DFT computations, to locate the protonation site equally well.

* Corresponding author. Tel.: +31 30 6096999; fax: +31 30 6031204.
E-mail address: joso@rijnh.nl (J. Oomens).

1387-3806/$ – see front matter © 2006 Elsevier B.V. All rights reserved.
doi:10.1016/j.ijms.2005.12.034

The IR photo-dissociation studies can roughly be divided into two groups: one where with a relatively low intensity laser a weakly bound messenger atom is detached, and one where with the use of powerful lasers, the ionic molecule itself is dissociated through the absorption of multiple photons. The experiments belonging to the second group are almost exclusively carried out in ion traps, where the parent ion is first mass selectively isolated and IR induced fragments are subsequently detected in the mass analyzer. This strategy is similar to the one used in extenso by Lifshitz and co-workers, in her studies of the dissociation behavior of molecular ions following electronic excitation [35,36]. The rate of internal energy conversion plays an extremely important role in this behavior; when it is relatively slow, dissociation may occur on electronically excited potential energy surfaces, which may be markedly different from those originating from the electronic ground state. The understanding of the resulting non-statistical dissociation behavior has been one of the major achievements of the work of Lifshitz [37]. Unlike electronic excitation, pure vibrational excitation, as is used in IR multiple photon dissociation (IRMPD), involves only the ground electronic state. Here, energy randomization is governed by intramolecular vibrational redistribution (IVR) and the associated relaxation rates are in general very fast for polyatomic molecules. Therefore, IR induced fragmentation is commonly believed to follow statistical unimolecular dissociation behavior. In IRMPD spectroscopy, this is of importance since it allows one to assume that dissociation rates depend only on the internal energy distribution obtained and not on the particular vibration that was excited. Thus, relative intensities in the observed spectrum can be considered to be meaningful.

There has been much interest in the spectroscopy and structure of nitrogen containing aromatic heterocycles (5/6 rings) mainly because of their close resemblance to various biochemically relevant compounds, particularly to the nucleic acid bases adenine and guanine and to the amino acid tryptophane. The gas-phase spectrum of indazole, $C_7H_6N_2$ (see Fig. 1), has been studied throughout the microwave, infrared, visible, and ultraviolet wavelength ranges [38–42]. A central question in these studies has been the 1H–2H tautomerization, i.e., the N1–N2 hydride shift (see structures **A** and **B** in Fig. 1). Based on these spectroscopic studies as well as on thermodynamical studies [43], the 1H-tautomer was determined to be more stable both in the electronic ground state as well as in the first electronically excited ($\pi\pi^*$) state. This was rationalized by the higher aromaticity of 1H-indazole, making this form energetically more favorable than 2H-indazole by 2–4 kcal/mol [38,43,44].

To the best of our knowledge, no infrared data for the charged species have been reported to date. A mass-analyzed threshold ionization (MATI) spectrum of indazole, giving information on the vibrational structure in the cation, was very recently reported [45]. Here, we present infrared spectra for protonated indazole as well as for bare cationic indazole and compare these to the spectrum of neutral indazole [39]. Despite the fact that the hydrogen stretching modes, which would obviously be quite different for the protonated species, are not probed in this study, the spectra are found to be very distinct. The mid-infrared spectral range investigated mainly contains the more delocalized heavy atom stretching modes of the C/N skeleton, as well as some hydrogen bending modes. Apparently, the relatively small changes in electron densities leave a strong imprint on the vibrational spectrum.

2. Experimental

The infrared spectra are obtained via free electron laser (FEL) induced multiple photon dissociation spectroscopy of the ions stored in an ion trap. The experimental apparatus, described in detail elsewhere [32], consists of a Paul-type quadrupole ion trap [46] coupled to a time-of-flight mass spectrometer. It follows the original design of Lubman and co-workers [47] that was also used in many of the studies of Lifshitz and co-workers [35]. Vapor-phase indazole is non-resonantly ionized using an ArF excimer laser, which is focused in the center of the ion trap, where the indazole ions and its ionic photo-fragments are instantaneously trapped. A mass spectrum taken immediately after the UV laser pulse, shown in Fig. 2A, indicates that extensive fragmentation occurs. Storing the ions for longer times, e.g., 100 ms, the amount of indazole ions recovers due to charge transfer from the low-mass ionic fragments to the abundantly present neutral indazole (see Fig. 2B). Moreover, a peak at mass 119, corresponding to protonated indazole or *indazolium*, arises due to proton transfer from ionic fragments to neutral indazole [48].

As the ions with mass 118 and 119 are the heaviest species present in the trap, they can be easily isolated from the lower mass peaks by temporarily (2 ms) increasing the amplitude of the RF trapping voltage, which raises the low-mass cut-off of the trap to just below mass 118 (see Fig. 2C). The ions are then irradiated with a pulse from the Free Electron Laser for Infrared eXperiments (FELIX [49]). FELIX delivers high energy ($\approx$100 mJ) infrared pulses of 5 μs duration, continuously tunable from 3 to 250 μm and with a bandwidth of approximately 0.4% of the central wavelength. Here, we record spectra in the 600–1800 cm^{-1} range.

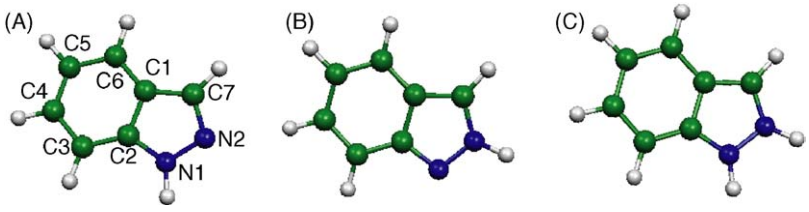

Fig. 1. Computed structures of cationic indazole species considered in this study: (**A**) 1H-indazole, (**B**) 2H-indazole, and (**C**) protonated indazole. The heavy atom numbering used in this work is given. We refer to N2 as the pyridine-like nitrogen and to N1 as the pyrrole-like nitrogen.

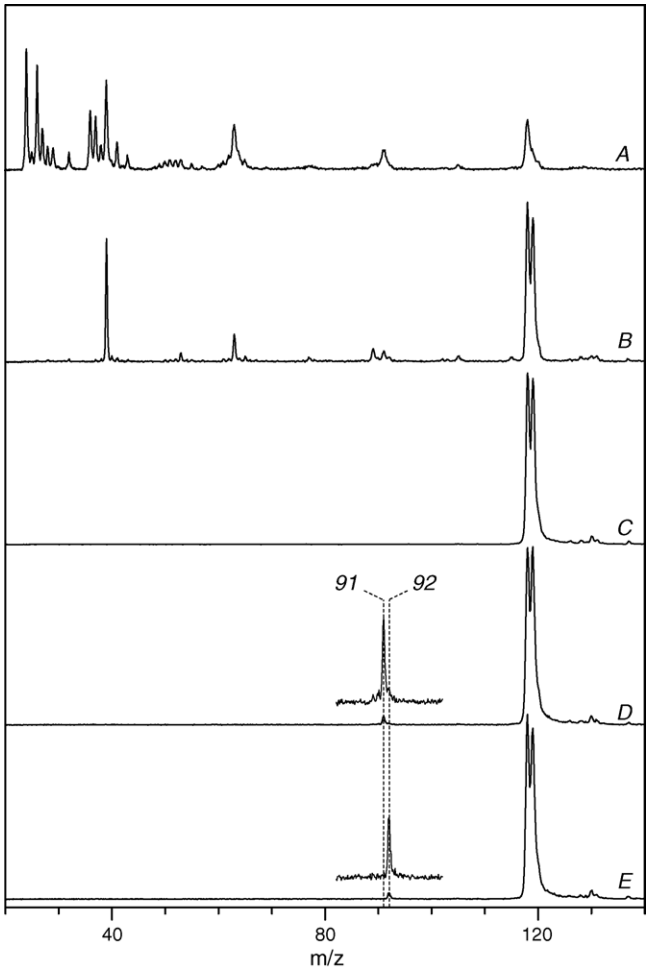

Fig. 2. Mass spectrum of cationic indazole and UV induced fragment ions taken directly after the ionization laser pulse (A) and after a reaction delay of 100 ms (B). Isolation of $m/z = 118$ and 119 corresponding to the indazole cation ($INDZ^+$) and protonated indazole ($INDH^+$), respectively (C). Wavelength-dependent IR multiple photon dissociation at 8.3 μm (D) and at 9.5 μm (E), corresponding to resonances in $INDZ^+$ and $INDH^+$.

Upon resonance, the ions are able to absorb multiple infrared photons, so that their internal energies reach levels beyond the dissociation threshold. Fragmentation is observed into mass channels 91 and 92, presumably corresponding to loss of an HCN unit from cationic and protonated indazole, respectively. Different spectral responses are found in the two mass channels (see Fig. 2D and E). Although the fragmentation yield is relatively small, a reasonable signal-to-noise ratio is achieved on account of the background free nature of the experimental method.

The experimental spectra are compared to theoretical spectra calculated using the B3LYP density functional and the D95(d,p) basis set. This method has been shown to give reliable results for a number of cationic polyaromatic species [32]. The spectrum of the neutral indazole molecule is also calculated, at the same level of theory, and the resulting spectrum is compared to the experimental vapor-phase spectrum of Cané et al. [39]. The strongest bands in the spectra are used to scale the DFT calculated frequencies, giving an empirical scaling factor of 0.972, which is subsequently used to scale the theoretical spectra of the charged species as well. Atomic charges in the molecules are calculated using the Atoms in Molecules (AIM) method as implemented in Gaussian98.

3. Results and discussion

The mass resolution of the ion trap, which is just sufficient to resolve the 118 and 119 mass peaks in the TOF trace (see Fig. 2), is insufficient to selectively isolate one of the two species. Therefore, the IR photo-dissociation spectra of the protonated and cationic indazole molecule are recorded simultaneously, where it is assumed that the cationic molecule dissociates solely into mass channel 91 and the protonated molecule solely into $m/z = 92$, and that there is no cross-talk between the two channels. This assumption can be justified by the observation that the two fragment channels show independent spectral responses (vide infra) and the identification of the fragment channels is a posteriori justified by comparison to DFT calculated spectra of the respective species. Below, we will first discuss the IR spectra of the two species individually and then compare them to each other and to the spectrum of the neutral indazole molecule.

3.1. Cationic indazole

The spectrum of the indazole cation together with the DFT calculated spectrum, convoluted with a 30 cm^{-1} FWHM Lorentzian line shape, is shown in Fig. 3. Band positions listed in Table 1 were determined by (manually) deconvoluting the spectrum with a Lorentzian lineshape function. This procedure is estimated to give IRMPD band positions to approximately ±3 cm^{-1} accuracy.

A reasonable agreement with the 1H-indazole calculation is obtained for the high-frequency end of the spectrum above 1000 cm^{-1}. The strongest band in the spectrum observed at 1207 cm^{-1} can be assigned to the asymmetric breathing mode of the two rings. Toward the blue end of the spectrum, a fairly broad asymmetrically shaped feature is observed, which is due to overlapping modes of mainly in-plane hydrogen bending and heavy atom stretching character. The NN stretching mode can still be discerned at 1078 cm^{-1}, but further to the red, the DFT calculation apparently fails to accurately predict the experimental spectrum. In the 800–1000 cm^{-1} range, two weak bands are observed, which may be due to three partly overlapping modes as calculated, however, the observed intensity ratio is not in agreement with theory. Finally, a strong feature is observed around 730 cm^{-1}, which seems to consist of more than one band. Assignment of this feature to overlapping CH and NH out-of-plane bending modes is questionable, particularly for the latter mode (721 cm^{-1} observed versus 669 cm^{-1} calculated). This discrepancy may be speculated to be due to problems of harmonic DFT calculations with out-of-plane NH bending modes, as has previously been noted for neutral indazole [39,41] as well as for several aniline-like systems [50]. However, another assignment of the entire spectrum is possible.

The substantial discrepancies between experiment and theory may raise the question whether ionization has induced rearrange-

Table 1
Infrared spectrum of the indazole cation

Observed		1H-indazole				2H-indazole			
ν	I^a	C_s	ν^b	$I^{c,d}$	Description[e]	C_s	ν^b	$I^{d,f}$	Description[e]
≈538	0.10	a''	601	0.16	β'_{CNN}	a''	558	0.13	β'_{CNN}
721	0.37	a''	669	0.51	β'_{NH}	a''	699	0.87	β'_{NH}
754	0.38	a''	740	0.37	β'_{CH}	a''	752	0.92	β'_{CH}
892	0.22	a'	833	0.28	δ_{ring}	a'	895	0.31	δ_{5ring}
		a'	898	0.18	δ_{ring}				
950	0.12	a'	931	0.56	δ_{ring}	a'	1004	0.68	σ_{NN}
1078	0.18	a'	1090	0.58	$\sigma_{NN}\beta_{CH}$	a'	1063	0.19	$\beta_{CH}\sigma_{NN}$
						a'	1085	0.39	β_{CH}
1207	1.00	a'	1211	1.00	Asym. breath	a'	1204	0.56	$\beta_{CH}\sigma_{CC}$
						a'	1235	1.00	$\beta_{CH}\sigma_{CN}$
						a'	1266	0.23	$\beta_{CH}\sigma_{CN}\beta_{NH}$
1380	0.62	a'	1383	0.40	$\beta_{NH}\sigma_{CC}\beta_{CNN}$	a'	1367	0.40	$\beta_{CH}\sigma_{CC}\beta_{CNN}$
1435	0.35	a'	1417	0.31	β_{CH}	a'	1404	0.71	$\sigma_{CC}\beta_{CH}\beta_{NH}$
		a'	1425	0.19	$\beta_{CH}\beta_{NH}\sigma_{CN}\sigma_{CC}$	a'	1433	0.63	$\beta_{NH}\beta_{CH}$
1530	0.17	a'	1589	0.28	$\sigma_{CN}\beta_{NH}\beta_{CH}$	a'	1525	0.54	$\sigma_{CC}\beta_{CH}$
						a'	1555	0.64	$\sigma_{CC}\beta_{CH}$

[a] Relative.
[b] Scaled by 0.972.
[c] Intensity relative to 1211 cm^{-1} band (144 km/mol).
[d] Only bands with $I > 0.13$ are listed.
[e] β', out-of-plane bend; β, in-plane bend; δ, deformation; σ, stretch.
[f] Intensity relative to 1235 cm^{-1} band (78 km/mol).

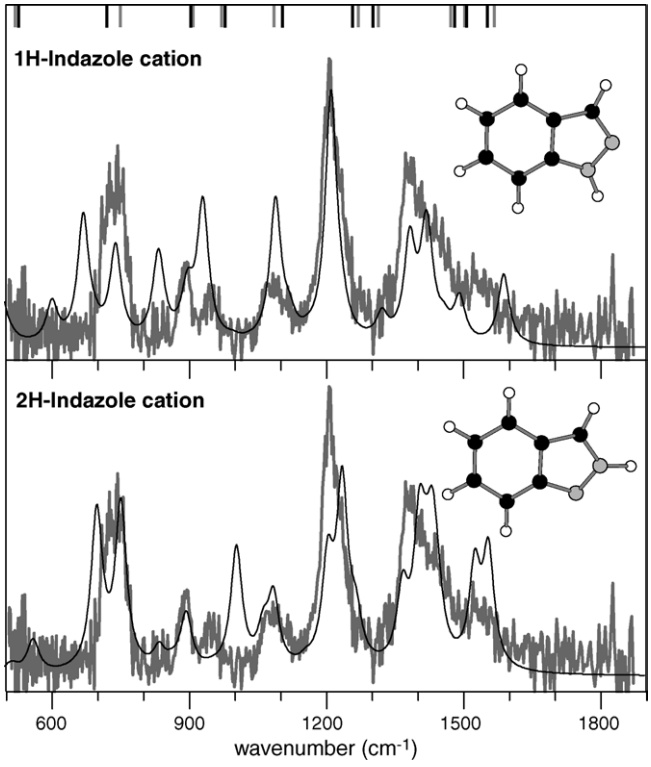

Fig. 3. Experimental IR spectrum of cationic indazole (grey) compared to the DFT calculated spectra for the 1H- and 2H-indazole cation tautomers (black). Vibrational energies obtained from MATI experiments (grey) and computed at the Hartree–Fock level (black), as reported by Su et al. [45], are indicated as sticks above our spectra.

Table 2
Calculated energies[a] of neutral and cationic indazole in 1H- and 2H-tautomeric forms

	Neutral		Cation		
	E (Hartree)	ΔE (eV)	E (Hartree)	ΔE (eV)	$^2A'$ (eV)[b]
1H	−379.8979	0	−379.6015	+0.215	0.93
2H	−379.8906	+0.199	−379.6094	0	1.47

[a] At the B3LYP/D95(d,p) level.
[b] Time-dependent DFT calculation. Relative to the respective $^2A''$ ground states.

ment, and in particular an N1–N2 hydride shift. Since the relative stability of neutral 1H-indazole with respect to 2H-indazole is believed to be due to its higher aromaticity and since the difference in energy is only a few kcal/mol [43,44], removal of an electron from the aromatic system may well change this delicate balance. A calculation of the 2H-indazole cation was therefore carried out giving an energy that is about 0.2 eV (5.0 kcal/mol) lower than that of the 1H-indazole cation, indicating that the relative stabilities of the 1H- and 2H-tautomers may indeed reverse upon ionization[1] (see Table 2). For both cationic tautomers, a time-dependent DFT calculation was performed to reassure the correctness of the $^2A''$ electronic ground states found by the B3LYP calculation. The first electronically excited states ($^2A'$) are on the order of 1 eV higher in energy (see Table 2), which appears to be far enough to conclude that the correct ground state configurations are considered.

[1] A calculation of the neutral species at the same level of theory favors the 1H-indazole by 0.21 eV (4.6 kcal/mol), which is fairly close to the value of 3.6 kcal/mol obtained at the MP2 level of theory by Catalán et al. [44].

The computed spectrum for the 2H-indazole cation is plotted onto the experimental spectrum in the second panel of Fig. 3. It appears to give a better match than the spectrum calculated for the 1H-indazole, e.g., for the low intensity modes in the 800–1100 cm^{-1} range and for the position of the bands in the 1500–1600 cm^{-1} range. More importantly, the out-of-plane NH bending mode, which is likely one of the most diagnostic modes distinguishing the two tautomers, observed at ≈721 cm^{-1}, is much better reproduced. On the other hand, however, the 2H-indazole calculation predicts a band at 1004 cm^{-1} having mainly NN stretching character, which is not observed experimentally. Hence, although both theory and experiment seem to suggest that the indazole cation is in the 2H tautomeric form as opposed to the neutral indazole molecule, it is difficult to definitively make this conclusion based on the present data.

A MATI spectrum of indazole, yielding the vibrational energies in the ground electronic state of the cation, was recently reported [45]. Comparison of the present infrared spectrum to the MATI spectra is difficult since in the MATI spectra, the observed intensities strongly depend on the S_1 intermediate vibronic level used. Furthermore, intensities are influenced by the overlap integral (Franck–Condon factor) and by the efficiency of the pulsed field ionization [45]. We have nonetheless plotted the level positions observed in the MATI spectra as sticks in Fig. 3. We should also mention apparent discrepancies in the computed spectra, obtained at the B3LYP level in this study and at the Hartree–Fock level in ref. [45]. It may be noted here that, in order for the overlap to be non-vanishing, the MATI technique likely probes the 1H-tautomer cation spectrum, even if the 2H would be lower in energy. This is opposed to our method, where non-resonant ionization, charge transfer reactions, as well as collisions allow for rearrangement processes.

3.2. Protonated indazole

Various sites of protonation have been theoretically investigated and the relative energies at the B3LYP/D95(d,p) level are given in Table 3. Clearly protonation at the pyridine-like nitrogen (N2 in Fig. 1) appears to be favored over all other protonation sites, which all lie about 1 eV (or about 100 kJ/mol) higher in energy. Protonation at the face of the aromatic ring (π-interaction) was also attempted but no stable minimum was found. Although many metal cations, e.g., alkali metal cations, are known to form stable π-bound complexes with aromatic molecules, protonation at the π-cloud is known to yield only saddle point structures [16,18].

Table 3
Computed energies (B3LYP/D95(d,p)) for different protonation sites

Site[a]	E (Hartree)	ΔE (eV)
N1	−380.2249	0.94
N2	−380.2595	0
C3	−380.2242	0.96
C4	−380.2155	1.20
C5	−380.2258	0.92
C6	−380.2183	1.12
C7	−380.2251	0.94

[a] See Fig. 1 for atom numbering.

Atomic charges calculated using the AIM method actually indicate that the pyrrole-like nitrogen atom N1 is more negative than N2. However, this is mainly due to attraction of electron density from the H atom. If the charges of the H atoms are summed into the heavy atoms, the net charges on N1 and N2 become $-0.37e$ and $-0.70e$, respectively, which rationalizes the N2 protonation site to yield the lowest energy structure.

The experimental spectrum of protonated indazole is shown in Fig. 4, and is compared to frequency calculations performed for the optimized structures of Table 3. The two main bands in the experimental spectrum, at 749 and 1046 cm^{-1}, appear to be very diagnostic in determining the protonation site: the only calculated structure that matches these two bands simultaneously is the N2 protonated structure. The rest of the spectrum also matches this structure reasonably well, except for the intensity of the band at the red end of the spectrum. Inspecting the calculations carefully, this mode is found to possess mainly out-of-plane NH bending character, which may be particularly anharmonic as discussed above. We therefore conclude that protonation occurs predominantly on the pyridine nitrogen atom, N2, yielding the structure depicted in Fig. 1.

Spectral assignments for protonated indazole based on the N2 protonated calculated spectrum are given in Table 4. The

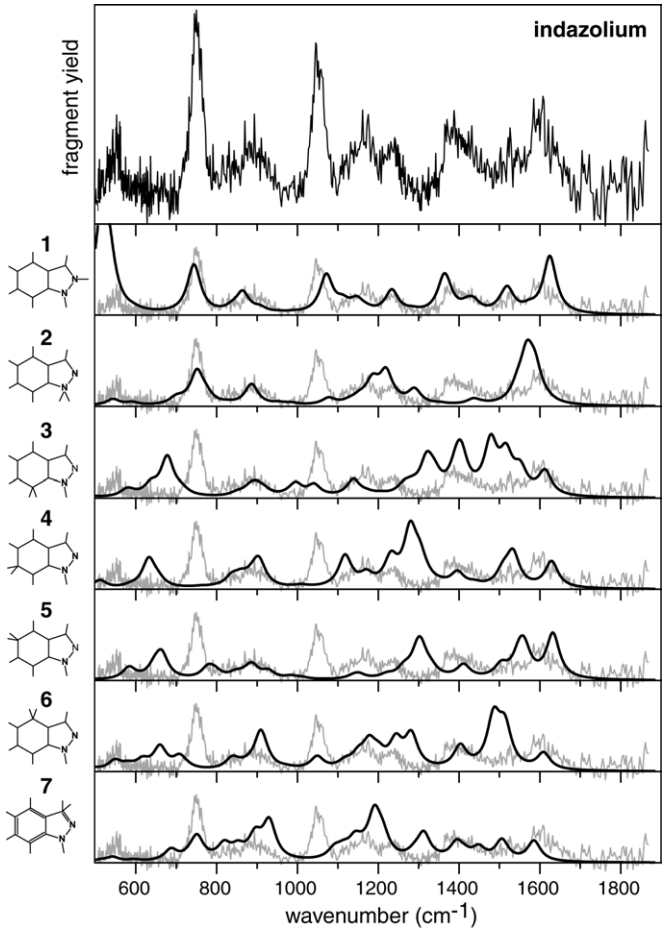

Fig. 4. IR spectrum of protonated indazole compared to DFT calculated spectra for different protonation sites.

Table 4
Infrared spectrum of protonated indazole

Observed		DFT calculated			
ν	I[a]	$\Gamma(C_s)$	ν[b]	I[c,d]	Description[e]
552	0.35	a''	517	134 (1.00)	β'_{NH}
		a''	534	53 (0.40)	$\beta'_{NH}\beta'_{CH}$
749	1.00	a''	744	60 (0.45)	β'_{CH}
832	0.10	a''	837	5 (0.04)	β'_{CH}
890	0.30	a''	864	26 (0.19)	β'_{CH}
1046	0.92	a'	1071	52 (0.39)	$\sigma_{CN}\sigma_{NN}$
1130	0.10	a'	1112	12 (0.09)	β_{CH}
1168	0.40	a'	1147	16 (0.12)	β_{CH}
1230	0.26	a'	1234	30 (0.22)	$\beta_{CH}\beta_{NH}$
1375	0.42	a'	1362	39 (0.29)	$\beta_{CH}\beta_{NH}$
		a'	1370	16 (0.12)	$\beta_{CH}\sigma_{CC}$
1422	0.25	a'	1419	8 (0.06)	$\beta_{CH}\beta_{NH}\sigma_{CN}\sigma_{CC}$
		a'	1435	13 (0.10)	$\beta_{NH}\beta_{CH}$
1523	0.24	a'	1520	32 (0.24)	$\sigma_{CN}\sigma_{CC}\beta_{CH}\beta_{NH}$
1595	0.48	a'	1625	79 (0.59)	$\sigma_{CC}\sigma_{CN}\beta_{CH}\beta_{NH}$

[a] Relative.
[b] Scaled by 0.972.
[c] In km/mol. Relative in parentheses.
[d] Only bands with $I > 5$ km/mol are listed.
[e] β', out-of-plane bend; β, in-plane bend; δ, deformation; σ, stretch.

two strongest bands in the spectrum at 749 and 1046 cm^{-1} are associated with the collective CH out-of-plane bending mode and the mode having mainly CN and NN stretching character, respectively. The remainder of the spectrum shows basically five relatively weak and broader features, of which the ones around 1200 and 1400 cm^{-1} can clearly be seen to consist of more than one band. These somewhat unresolved structures are in quite good agreement with the computations so that the assignments of mainly heavy atom stretching modes around 1600 cm^{-1} and mainly in-plane hydrogen bending modes around 1200 and 1400 cm^{-1} seem justified.

3.3. Comparison

The spectra for the neutral, protonated, and cationic indazole molecule are compared to each other in Fig. 5. For the neutral species, the DFT calculation is shown, which has been checked to be in good agreement with the experimental gas-phase spectrum of Cané et al. [39]. Making spectral comparisons based on the calculated normal modes one should be cautious because the modes have in general a quite delocalized character, particularly the in-plane skeletal modes above ≈900 cm^{-1}, and therefore, a clear one-to-one correlation is often not possible, even for such similar systems. Some general trends can nonetheless be noticed.

Particularly for the neutral and protonated species, which are of course *iso*-electronic, spectral similarities can be recognized. In the low energy range, the bands with CH out-of-plane bending character can be fairly easily correlated, as indicated by the dotted lines in Fig. 5. To the blue, in the 900–1100 cm^{-1} range, bands have NN and CN stretching and bending character, and here clear differences are observable due to the attachment of the proton to one of the N atoms. In the high energy range of the

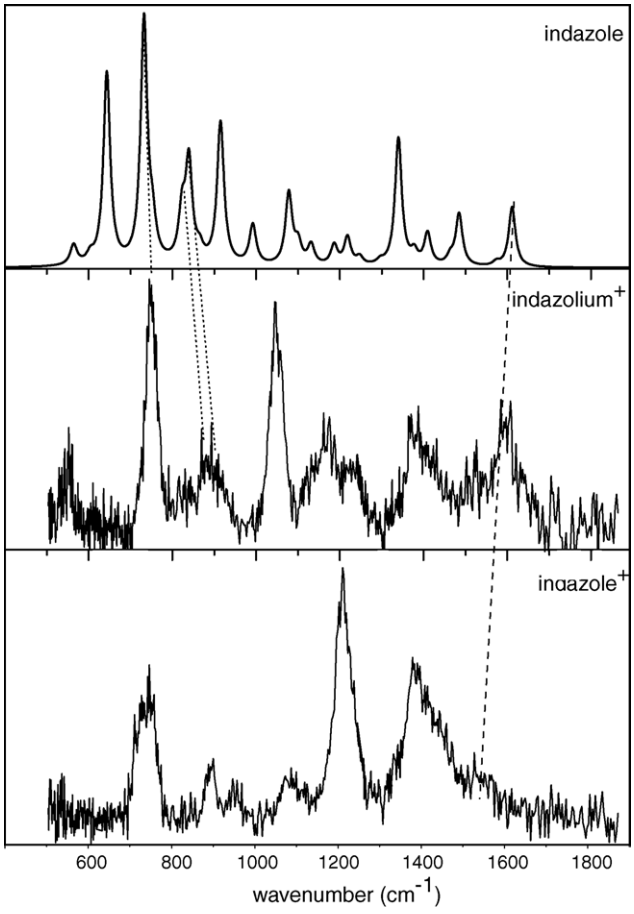

Fig. 5. Comparison of the infrared spectra of neutral, protonated, and cationic indazole. CH out-of-plane bending modes in the neutral and protonated molecule are connected by dotted lines. The observed trend in band positions of the mode(s) containing CC stretching character is indicated by the dashed line.

spectrum, three weaker features, roughly around 1400, 1500, and 1600 cm^{-1} are observed in both spectra (the central one is only weakly observed in the protonated indazole spectrum). Finally, the band around 650 cm^{-1} in the neutral spectrum, which is due to the out-of-plane NH bending is not reflected in the protonated species. As already mentioned, this may be due to the increased anharmonicity of this vibration [39,41], which not only makes a harmonic frequency calculation unreliable but which may also severely limit the efficiency of multiple photon excitation in our experiments [51].

The spectrum of the cationic species is quite different with a strong mode appearing around 1200 cm^{-1}. At the very blue end of the spectrum, there is clearly less intensity than in the protonated and neutral species, as if the bands were shifted toward lower frequencies. The modes in this range have mainly CC stretching character and their frequencies depend sensitively on the electron density in the aromatic cloud. Thus, the removal of an electron from the π-cloud [41,42] upon ionization causes a red-shift of those modes on the order of 50 cm^{-1}. This observation correlates nicely with the DFT computed average CC bond length in the six-membered ring, which is 1.408, 1.410, and 1.414 Å for the neutral, protonated, and (2H-)cationic molecule, respectively.

4. Conclusions

Gas-phase infrared spectra are presented for protonated as well as for cationic indazole. The spectra are compared to DFT computed spectra and to the spectrum of the neutral molecule. The protonation site of the molecule has been established to be the pyridine-like nitrogen atom, which is the most negatively charged site in the neutral molecule. The agreement between computed and experimental spectra is reasonable for the closed-shell species, the protonated and neutral molecule, but somewhat worse for the radical cation. This may be due to tautomerization from the 1H- to 2H-indazole form upon ionization, which is calculated to be energetically favorable at the B3LYP/D95(d,p) level of theory.

Acknowledgments

We would like to thank one of the reviewers for alerting us to the issue of tautomerism in indazole and we further thank Dr. G. Berden and Dr. E. Jalviste for helpful discussions on this subject. This work is part of the research program of FOM, which is financially supported by the Nederlandse Organisatie voor Wetenschappelijk Onderzoek (NWO). We highly appreciate the skillful assistance by the FELIX staff.

References

[1] E. Nir, K. Kleinermanns, M.S. de Vries, Nature 408 (2000) 949.
[2] T.S. Zwier, J. Phys. Chem. A 105 (2001) 8827.
[3] O.M. Cabarcos, C.J. Weinheimer, J.M. Lisy, J. Chem. Phys. 110 (1999) 8429.
[4] E.G. Robertson, J.P. Simons, Phys. Chem. Chem. Phys. 3 (2001) 1.
[5] M. Mons, I. Dimicoli, F. Piuzzi, B. Tardivel, M. Elhanine, J. Phys. Chem. A 106 (2002) 5088.
[6] L.C. Snoek, E.G. Robertson, R.T. Kroemer, J.P. Simons, Chem. Phys. Lett. 321 (2000) 49.
[7] J.M. Bakker, L. MacAleese, G. Meijer, G. von Helden, Phys. Rev. Lett. 91 (2003) 203003.
[8] R.A. Jockusch, F.O. Talbot, J.P. Simons, Phys. Chem. Chem. Phys. 5 (2003) 1502.
[9] C. Unterberg, A. Gerlach, T. Schrader, M. Gerhards, J. Chem. Phys. 118 (2003) 8296.
[10] W. Chin, I. Compagnon, J.P. Dognon, C. Canuel, F. Piuzzi, I. Dimicoli, G. von Helden, G. Meijer, M. Mons, J. Am. Chem. Soc. 127 (2005) 1388.
[11] I. Compagnon, J. Oomens, J. Bakker, G. Meijer, G. von Helden, Phys. Chem. Chem. Phys. 7 (2005) 13.
[12] L.C. Snoek, T. van Mourik, J.P. Simons, Mol. Phys. 101 (2003) 1239.
[13] M.A. Duncan, Int. J. Mass Spectrom. 200 (2000) 545.
[14] T. Oka, Phys. Rev. Lett. 45 (1980) 531;
C.S. Gudeman, M.H. Begemann, J. Pfaff, R.J. Saykally, Phys. Rev. Lett. 50 (1983) 727;
M. Okumura, L.I. Yeh, Y.T. Lee, J. Chem. Phys. 83 (1985) 3705.
[15] N. Solcà, O. Dopfer, Chem. Phys. Lett. 342 (2001) 191.
[16] N. Solcà, O. Dopfer, Angew. Chem. Int. Ed. 10 (2002) 3628.
[17] N. Solcà, O. Dopfer, J. Am. Chem. Soc. 125 (2003) 1421.
[18] W. Jones, P. Boissel, B. Chiavarino, M.E. Crestoni, S. Fornarini, J. Lemaire, P. Maître, Angew. Chem. Int. Ed. 42 (2003) 2057.
[19] Y. Inokuchi, N. Nishi, J. Phys. Chem. A 107 (2003) 11319.
[20] B. Lucas, G. Grégoire, J. Lemaire, P. Maître, J.M. Ortega, A. Rupenyan, B. Reimann, J.P. Schermann, C. Defrancois, Phys. Chem. Chem. Phys. 6 (2004) 2659.
[21] J. Oomens, G. von Helden, G. Meijer, J. Phys. Chem. A 108 (2004) 8273.
[22] B. Lucas, G. Grégoire, J. Lemaire, P. Maître, F. Glotin, J.P. Schermann, C. Defrancois, Int. J. Mass Spectrom. 243 (2005) 105.
[23] B. Chiavarino, M. Crestoni, S. Fornarini, J. Lemaire, L. Mac Aleese, P. Maître, ChemPhysChem 6 (2005) 437.
[24] H.-B. Oh, C. Lin, H.Y. Hwang, H. Zhai, K. Breuker, V. Zabrouskov, B.K. Carpenter, F.W. McLafferty, J. Am. Chem. Soc. 127 (2005) 4076.
[25] K.R. Asmis, N.L. Pivonka, G. Santambrogio, M. Brümmer, C. Kaposta, D.M. Neumark, L. Wöste, Science 299 (2003) 1375.
[26] D.T. Moore, J. Oomens, L. van der Meer, G. von Helden, G. Meijer, J. Valle, A.G. Marshall, J.R. Eyler, ChemPhysChem 5 (2004) 740.
[27] J.M. Headrick, J.C. Bopp, M.A. Johnson, J. Chem. Phys. 121 (2004) 11523; E.G. Diken, J.M. Headrick, J.R. Roscioli, J.C. Bopp, M.A. Johnson, A.B. McCoy, J. Phys. Chem. A 109 (2005) 1487.
[28] T.D. Fridgen, L. MacAleese, P. Maître, T.B. McMahon, P. Boissel, J. Lemaire, Phys. Chem. Chem. Phys. 7 (2005) 2747.
[29] O. Asvany, P.P. Kumar, B. Redlich, I. Hegemann, S. Schlemmer, D. Marx, Science 309 (2005) 1219.
[30] H. Oh, K. Breuker, S.K. Sze, Y. Ge, B.K. Carpenter, F.W. McLafferty, Proc. Natl. Acad. Sci. U.S.A. 99 (2002) 15863.
[31] J. Oomens, N. Polfer, D.T. Moore, L. van der Meer, A.G. Marshall, J.R. Eyler, G. Meijer, G. von Helden, Phys. Chem. Chem. Phys. 7 (2005) 1345.
[32] J. Oomens, A.J.A. van Roij, G. Meijer, G. von Helden, Astrophys. J. 542 (2000) 404;
J. Oomens, G. Meijer, G. von Helden, J. Phys. Chem. A 105 (2001) 8302.
[33] J.J. Valle, J.R. Eyler, J. Oomens, D.T. Moore, A.F.G. van der Meer, G. von Helden, G. Meijer, C.L. Hendrickson, A.G. Marshall, G.T. Blakney, Rev. Sci. Instrum. 76 (2005) 023103.
[34] J. Lemaire, P. Boissel, M. Heninger, G. Mauclaire, G. Bellec, H. Mestdagh, A. Simon, S.L. Caer, J.M. Ortega, F. Glotin, P. Maître, Phys. Rev. Lett. 89 (2002) 273002.
[35] W. Cui, B. Hadas, B. Cao, C. Lifshitz, J. Phys. Chem. A 104 (2000) 6339.
[36] Y. Hu, B. Hadas, M. Davidovitz, B. Balta, C. Lifshitz, J. Phys. Chem. A 107 (2003) 6507.
[37] C. Lifshitz, J. Phys. Chem. 87 (1983) 2304.
[38] B. Velino, E. Cané, A. Trombetti, G. Corbelli, F. Zerbetto, W. Caminati, J. Mol. Spectrosc. 155 (1992) 1.
[39] E. Cané, P. Palmieri, R. Tarroni, A. Trombetti, J. Chem. Soc., Faraday Trans. 89 (1993) 4005.
[40] G. Berden, W.L. Meerts, E. Jalviste, J. Chem. Phys. 103 (1995) 9596.
[41] E. Jalviste, F. Temps, J. Chem. Phys. 111 (1999) 3898.
[42] E. Cané, A. Trombetti, B. Velino, W. Caminati, J. Mol. Spectrosc. 155 (1992) 307.
[43] J. Catalán, J.C. del Valle, R.M. Claramunt, G. Boyer, J. Laynez, J. Gómez, P. Jiménez, F. Tomás, J. Elguero, J. Phys. Chem. 98 (1994) 10606.
[44] J. Catalán, J.L.G. de Paz, J. Elguero, J. Chem. Soc., Perkin Trans. 2 (1996) 57.
[45] H. Su, M. Pradhan, W.B. Tzeng, Chem. Phys. Lett. 411 (2005) 86.
[46] W. Paul, Rev. Mod. Phys. 62 (1990) 531.
[47] S.M. Michael, M. Chien, D.M. Lubman, Rev. Sci. Instrum. 63 (1992) 4277.
[48] J. Oomens, G. von Helden, G. Meijer, J. Phys. Chem. A 108 (2004) 8273.
[49] D. Oepts, A.F.G. van der Meer, P.W. van Amersfoort, Infrared Phys. Technol. 36 (1995) 297.
[50] W.E. Sinclair, D.W. Pratt, J. Chem. Phys. 105 (1996) 7942;
H. Piest, G. von Helden, G. Meijer, J. Chem. Phys. 110 (1999) 2010;
J. Oomens, D.T. Moore, G. Meijer, G. von Helden, Phys. Chem. Chem. Phys. 6 (2004) 710.
[51] J. Oomens, A.G.G.M. Tielens, B.G. Sartakov, G. von Helden, G. Meijer, Astrophys. J. 591 (2003) 968.